

DIGITAL VISCOELASTIC SEISMIC MODELS AND DATA SETS OF CENTRAL SAUDI ARABIA IN THE PRESENCE OF NEAR-SURFACE KARST FEATURES

ABDULLATIF A. AL-SHUHAIL¹, ABDULLAH A. ALSHUHAIL¹, YEHIA A. KHULIEF², OLUSEUN A. SANUADE¹, AYMAN F. AL-LEHYANI¹, SEPTRIANDI A. CHAN¹, ABDUL LATIF ASHADI¹, MOHAMMED ZIA ULLAH KHAN³, SIKANDAR KHAN², ADNAN M. ALMUBARAK¹, SALEM G. AL-JUHANI¹ and SYED ABDUL SALAM³

¹ *Geosciences Department, King Fahd University of Petroleum & Minerals (KFUPM), Dhahran 31261, Saudi Arabia. ashuhail@kfupm.edu.sa*

² *Mechanical Engineering Department, King Fahd University of Petroleum & Minerals (KFUPM), Dhahran 31261, Saudi Arabia.*

³ *Electrical Engineering Department, King Fahd University of Petroleum & Minerals (KFUPM), Dhahran 31261, Saudi Arabia.*

(Received September 19, 2018; revised version accepted October 30, 2019)

ABSTRACT

Al-Shuhail, A.A., Alshuhail, A.A., Khulief, Y.A., Sanuade, O.A., Al-Lehyani, A.F., Chan, S.A., Ashadi, A.L., Khan, M.Z.U., Khan, S., Almubarak, A.M., Al-Juhani, S.G. and Salam, S.A., 2020. Digital viscoelastic seismic models and data sets of central Saudi Arabia in the presence of near-surface karst features. *Journal of Seismic Exploration*, 29: 15-28.

Central Saudi Arabian fields are generally known for their high-quality light oil that derives from structural and stratigraphic traps. Despite their unique geological settings, there are no existing digital geological models or synthetic seismic data that are publicly available for testing hypotheses and algorithms. We attempt to fill this gap by compiling 2D viscoelastic models of one of these fields and generate corresponding multi-component synthetic seismic data sets. We selected the Usaylah field because its oil production comes interestingly from a stratigraphic trap in the Permian siliciclastic Unayzah reservoir. Furthermore, to simulate realistic central Arabian near-surface conditions, we generate two models: one with and another without karst features in the top Aruma limestone.

The P-wave velocities and densities of the entire stratigraphic column from basement to Aruma limestone were compiled from public sources. We then calculate S-wave velocities from P-wave velocities using empirical V_S - V_P relations that we established and generalized from few published well logs. P-wave and S-wave quality factors were also calculated from the corresponding P-wave and S-wave velocities using an empirical square-root formula. A total of four synthetic 2D seismic data sets comprising the horizontal and vertical components excluding and including karst features were generated using a finite-difference algorithm. We share the models and seismic data sets publicly hoping that this will motivate interested researchers to test their research ideas.

KEY WORDS: viscoelastic model, Usaylah field, karst feature.

INTRODUCTION

The Usaylah field is located in central Saudi Arabia about 175 km south of Riyadh. This field is the 14th oil and gas field discovered in central Saudi Arabia in which the production of hydrocarbon comes from the upper part of the Permian Unayzah Formation (Evans et al., 1997). The field is geologically situated on the eastern flank of the Hawtah Trend, one of the two prominent structural trends in central Saudi Arabia: Nuayyim and Hawtah. The trends are established by the reactivation of basement structures during the Hercynian Orogeny (Late Devonian to Carboniferous), opening and closing of Neo-Tethys (Triassic to Late Cretaceous), and Tertiary collision (Al-Husseini, 2004). Fig. 1 shows the location of the Usaylah field.

Most of the fields discovered in the region are structural traps (anticlines). However, the Usaylah field is reported as the first purely stratigraphic trap discovered in central Saudi Arabia (Evans et al., 1997). The prospect was successfully mapped using a 3D seismic survey by Saudi Aramco. The type of stratigraphic trap for this field is isolated reservoir sands that pinch-out in the updip section to the west and form stratigraphic traps along the eastern flank of the Hawtah anticline.

McGillivray and Husseini (1992) classified the Unayzah formation in the Hawtah and Hazmiyah fields into two members: Unayzah-A and Unayzah-B. These members are separated by either red-brown siltstones or fine-grained silty sandstones. Melvin and Sprague (2006) carried out studies on the provenance and stratigraphy of sediments in Permian–Carboniferous lower Unayzah sandstones in eastern-central of Saudi Arabia. They divided the sandstones of the Lower Unayzah into Unayzah-C (the lowermost unit comprised of quartzose sandstones), Unayzah-B (mainly made of glaciogenic sediments), and unnamed middle Unayzah members made up of essentially fine-grained red beds.

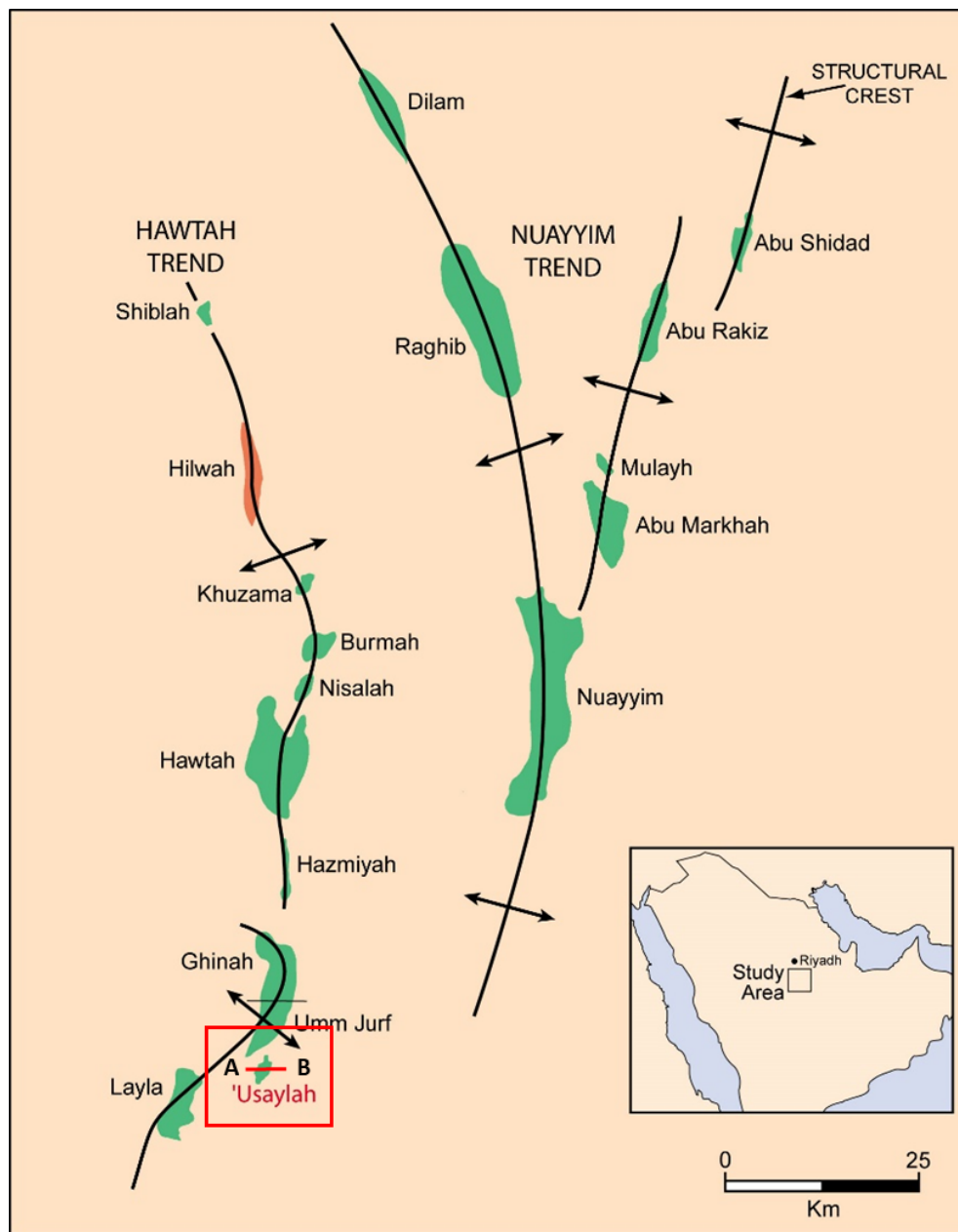


Fig. 1. Map showing the Usaylah field (red box). Approximate location of the compiled 2D model is indicated by the line AB (modified from Evans et al., 1997).

Macrides and Kelamis (2000) carried out a pilot 9C, 2D experiment which consisted of three seismic profiles in central Saudi Arabia. The aim of their study was to delineate variations in lithology within the Unayzah reservoir. The low ratio of V_p to V_s in the Unayzah field was interpreted to show the presence of high clean sands while high ratios were interpreted to show silty sand and shale. Well logs were used to validate the result of the seismic interpretation. They stated that variations in average ratio of V_p to

V_S calculated from P-P and S-S isochrons for the carbonate Khuff and clastic Unayzah, describe the changes in lithology within them.

Fournier et al. (2002) carried out a detailed lithostratigraphic interpretation using 3D and 2D seismic data sets of the Upper Unayzah formation in central Saudi Arabia, with the objective to describe reservoir variations between wells. Seismic facies analysis on the 3D data set was used to identify a sand-prone facies in the Upper Unayzah. The amount of sands and average porosities were also estimated using quantitative statistical calibration of seismic attributes. The results of seismic attributes confirm the results of the seismic facies analysis. Seismic facies analysis on the 2D seismic lines was used to identify prospects east of the Layla 3D area, with evidence of a sand-prone facies in the Upper Unayzah, which agrees with the result of the 3D seismic facies analysis.

Knox et al. (2010) carried out a study on the assemblages of heavy minerals in the Unayzah reservoir sandstones of central Saudi Arabia in order to identify successive changes in provenance signature. They identified four members which are Unayzah C, Unayzah B, Unayzah A and the basal Khuff clastic. They attributed the changes in the mineralogical stratigraphy to successive developments in the geography and climate of the area and the pattern of sources and transportation of sand.

Al-Khidir et al. (2011) studied the sandstones of the Shajara Formation (Lower, Middle and Upper Shajara) of the Unayzah reservoir in the greater Arabian Basin. They employed mercury intrusion technique on the sandstone samples. The result of their analysis characterized the three sandstones as heterogeneous megaporous reservoirs with lower sand units as the best reservoir in terms of quality. Petrophysical description of the sandstone samples shows that the quality of the reservoir is controlled by the depositional facies and rock texture and the quality increases with an increase of grain size and grain sorting.

Despite their interesting subsurface and near-surface features, there exist no digital models nor synthetic seismic data sets for any central Saudi Arabian field that are available in the public domain. The objective of this study is to compile digital viscoelastic depth models and generate corresponding synthetic seismic data sets of one of these fields (i.e., Usaylah).

We use a viscoelastic wave equation that requires P-wave velocity (V_P), S-wave velocity (V_S), Density (ρ), P-wave quality factor (Q_P), and S-wave quality factor (Q_S) to generate 2D synthetic viscoelastic multi-component seismic data sets that include vertical and horizontal components recorded by surface geophones using a conventional 2D acquisition geometry.

Digital horizons, faults, karst features, viscoelastic models, and synthetic multi-component seismic data sets can be downloaded freely from the following link:

<https://www.dropbox.com/sh/r3u26nnqc7vtwyd/AAAAIdgwyFVlhNuN1WF-AolTa?dl=0>

A file containing horizons, faults, and karst features is provided in comma-separated-values (CSV) format while models and seismic data files are provided in Seismic Un*x (SU) format.

DEVELOPMENT OF DIGITAL DEPTH MODELS

We performed extensive literature review to construct realistic subsurface geophysical models of the Usaylah field. However, the number of published data on the field is very limited with no available source with a complete subsurface geological model covering Precambrian to Mesozoic succession in the Usaylah field, Saudi Arabia. Therefore, in this study, we compile one geologically and geophysically consistent model from many references that are available in the literature.

The geologic column in the Usaylah field consists of Mesozoic era, Paleozoic era, and a Precambrian Basement. Mesozoic era was subdivided into twelve main formations: Aruma (L-1), Wasia (L-2), Shuaiba (L-3), Biyadh (L-4), Hith (L-5), Arab (L-6), Hanifa and Tuwaiq Mountain (L-7), Dhurma (L-8), Marrat (L-9), Minjur (L-10), Jilh (L-11), and Sudair (L-12) formations. The Paleozoic era consists of five main formations including Khuff (L-13), Unayzah (L-14), Qusaiba (L-15), Qasim (L-16), and Saq (L-17) formations. The lowermost layer in our model is the Precambrian Basement (L-18) that is assumed as a half space with an infinite thickness. Table 1 shows the average thickness, the lithology, P- and S-wave velocities, P- and S-wave quality factors, and densities of each Formation in the Usaylah field model. Eventually, eighteen layers and three major faults were defined and digitized at varying intervals. Table 2 shows P- and S-wave velocities, P- and S-wave quality factors, and densities of fluids filling karst features modeled within the topmost Aruma Formation. The horizons and faults are presented in Fig. 2.

Table 1. P- and S-wave velocities, P- and S-wave quality factors, and densities of layers of the Usaylah field model.

Layer No.	Formation	Average Thickness (m)	Lithology	V_p (m/s)	ρ (kg/m ³)	V_s (m/s)	Q_p	Q_s
L-1	Aruma	160	Limestone	2730.0 ^a	2091.0 ^a	1672.1 ^c	52.25 _i	40.89 _i
L-2	Wasia	230	Sandstone	3233.0 ^a	2277.0 ^a	2141.9 ^b	56.86 _i	46.28 _i
L-3	Shuaiba	100	Limestone	3010.0 ^a	2037.0 ^a	1817.7 ^c	54.86 _i	42.63 _i
L-4	Biyadh	320	Sandstone	4045.0 ^a	2364.0 ^a	2700.8 ^b	63.60 _i	51.97 _i
L-5	Hith	100	Anhydrite	4483.0 ^d	2960.0 ^d	2327.5 ^d	66.96 _i	48.24 _i
L-6	Arab	130	Limestone	5140.0 ^d	2400.0 ^d	2748.0 ^d	71.69 _i	52.42 _i
L-7	Hanifa & Tuwaiq Mountain	310	Limestone	5697.5 ^d	2550.0 ^d	2903.0 ^d	75.48 _i	53.88 _i
L-8	Dhurma	341	Limestone	5033.0 ^e	2458.0 ^e	2869.7 ^c	70.94 _i	53.57 _i
L-9	Marrat	146	Shale	3272.0 ^e	2410.0 ^e	1436.0 ^f	57.20 _i	37.89 _i
L-10	Miniur	350	Sandstone	3930.0 ^e	2394.0 ^e	2499.0 ^c	62.69 _i	49.99 _i
L-11	Jilh	293	Dolomite	4823.0 ^e	2400.0 ^e	2760.5 ^d	69.45 _i	52.54 _i
L-12	Sudair	100	Shale	5182.0 ^g	2372.0 ^g	2674.0 ^g	71.99 _i	51.71 _i
L-13	Khuff	180	Dolomite	4953.0 ^g	2705.5 ^g	2530.0 ^g	70.38 _i	50.30 _i
L-14	Unayzah	100	Sandstone	3752.0 ^g	2404.5 ^g	2085.0 ^g	61.25 _i	45.66 _i
L-15	Qusaiba	300	Shale	3898.0 ^g	2485.5 ^g	2143.0 ^g	62.43 _i	46.29 _i
L-16	Qasim	200	Sandstone	3685.0 ^h	2380.0 ^h	2453.0 ^c	60.70 _i	49.53 _i
L-17	Saq	300	Sandstone	3765.0 ^h	2350.0 ^h	2508.0 ^c	61.36 _i	50.08 _i
L-18	Basement	~	Igneous and metamorphic	6380.0 ^j	2800.0 ^j	3580.0 ^j	79.87 _i	59.83 _i

^aAlfaraj et al. (1998); ^bOur sandstone eq.; ^cAmeen et al. (2009) eq.; ^dLiu et al. (2013); ^eDasgupta, et al. (2002); ^fOur shale eq.; ^gMacrides and Kelamis (2000); ^hAl-Ahmadi (2009); ⁱMittet (2007), ^jMooney et al. (1985).

Table 2. P- and S-wave velocities, P- and S-wave quality factors, and densities of fluids filling the karst features within the topmost Aruma formation.

Karst filling	V_p (m/s)	V_s (m/s)	ρ (kg/m ³)	Q_p	Q_s
Water	1450	0	1000	100,000	100,000
Air	330	0	1.23	100,000	100,000

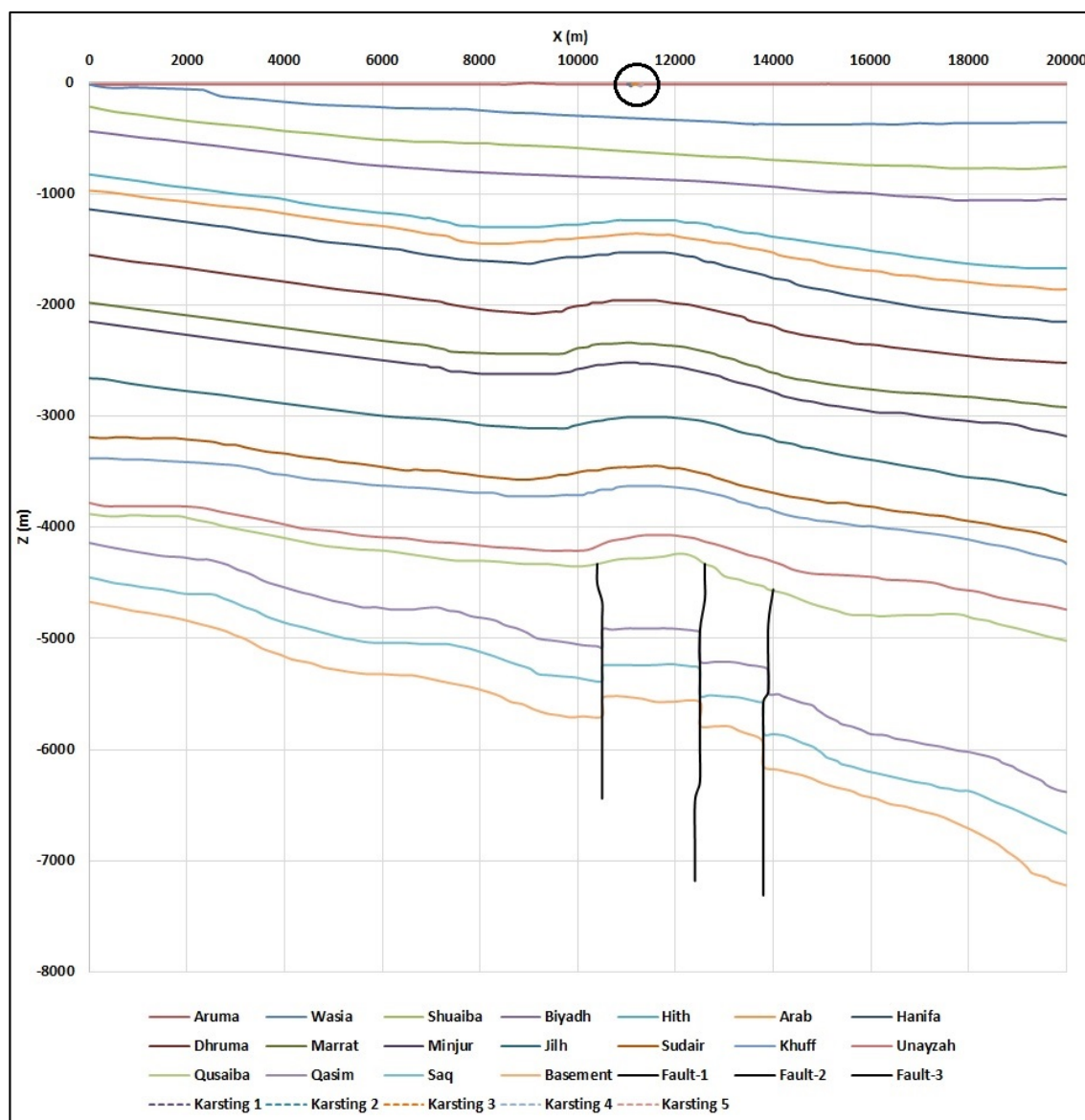


Fig. 2. Digitized model of the Usaylah field in Central Saudi Arabia. Locations of karst features are indicated by a circle between X=10,000 and 12,000 m.

The elastic properties such as P-wave velocities and densities of each layer were determined from well-log data available in Alfaraj et al. (1998), Macrides and Kelamis (2000), Dasgupta et al. (2002), Al-Ahmadi (2009), and Liu et al. (2013). However, just few S-wave velocities were reported in all these references. In order to complete the velocities of S-wave for the whole stratigraphic column, V_S - V_P relations for Saudi Arabian lithologies were used. For carbonates, we used the relation presented by Ameen et al. (2009) in eq. (1). For sandstones and shales, we use the relations in eqs. (2) and (3), respectively, that we developed from well-log data available in Macrides and Kelamis (2000). P- and S-wave velocities in eqs. (1)-(3) are expressed in units of m/s

$$V_S = 0.52V_P + 252.51 \quad (1)$$

$$V_S = 0.6882V_P - 83.009 \quad (2)$$

$$V_S = 0.4863V_P + 983.74 \quad (3)$$

P-wave and S-wave quality factors (Q_P and Q_S) were determined by using the formula proposed by Mittet (2007). This formula involved taking the square root of the corresponding value of V_P and V_S , respectively. The quality factors of karst-filling fluids are assumed to be infinite and were assigned a large value of 100,000 for modeling purposes. We note that although Figs. 3(a)-(e) show only the central part of the constructed viscoelastic models in the Usaylah field, the whole models (i.e., 20,000 m wide by 8,000 m deep) were used for the generation of the synthetic seismic data sets.

The central Saudi Arabian near-surface layer generally consists of carbonates that are easily weathered forming karst features that affect seismic surveys near them. To model these effects, we included five randomly shaped and closely distributed karst features in the uppermost Aruma limestone Formation. To add a realistic level of complexity to the model, two of these karst features are water-saturated while the others are filled with air. These karst features were absent in one instance of the model and present in another instance. Fig. 4 shows detailed viscoelastic models of the karst features.

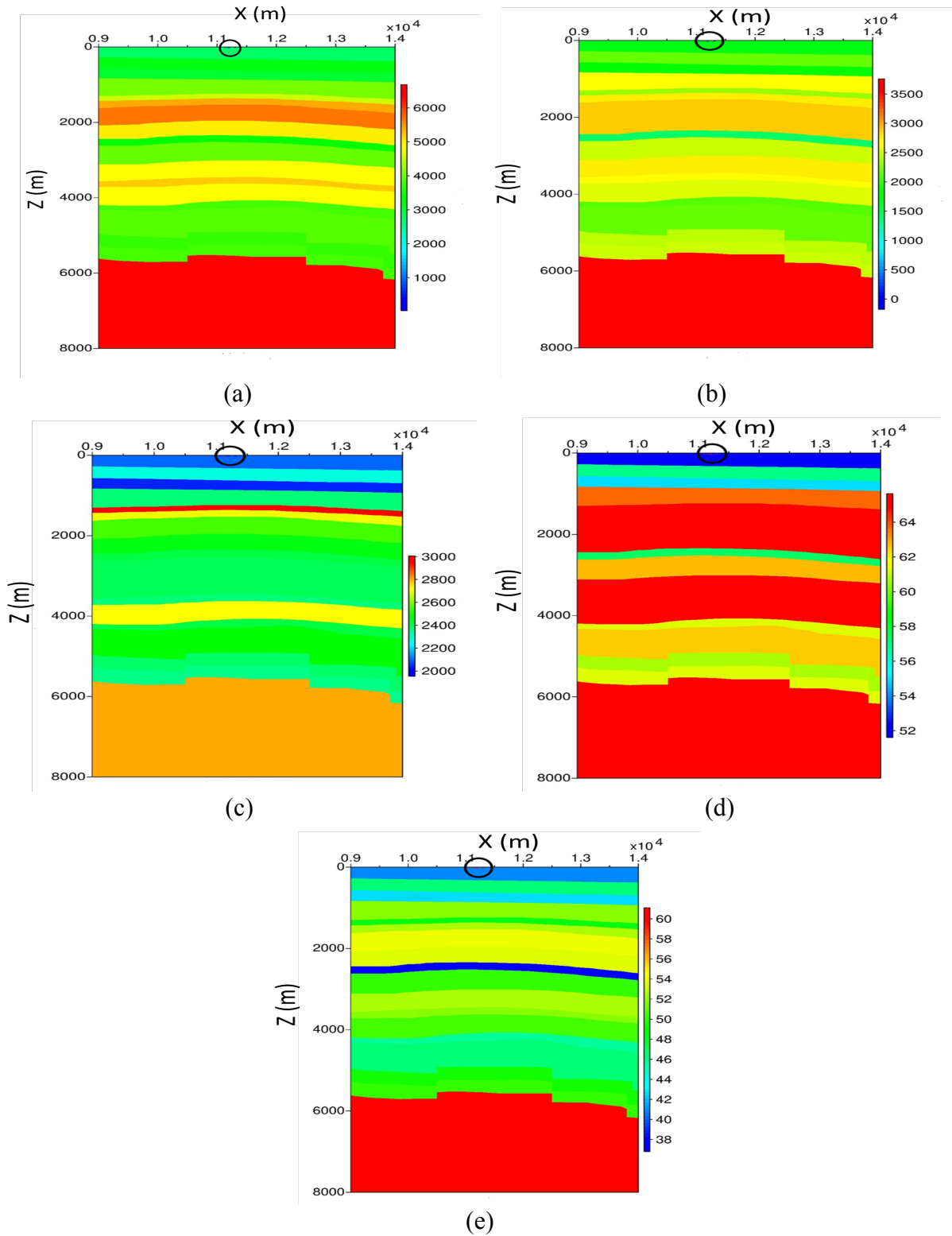


Fig. 3. (a) V_P model of the Usaylah field in central Saudi Arabia. Color scale shows velocity values in m/s. (b) V_S model. Color scale shows velocity in m/s. (c) Density model. Color scale indicates density values in kg/m^3 . (d) Q_P model. Color scale indicates quality factor values in dimensionless units. (e) Q_S model. Color scale indicates quality factor values in dimensionless units. Karst features are inside the circle of each figure.

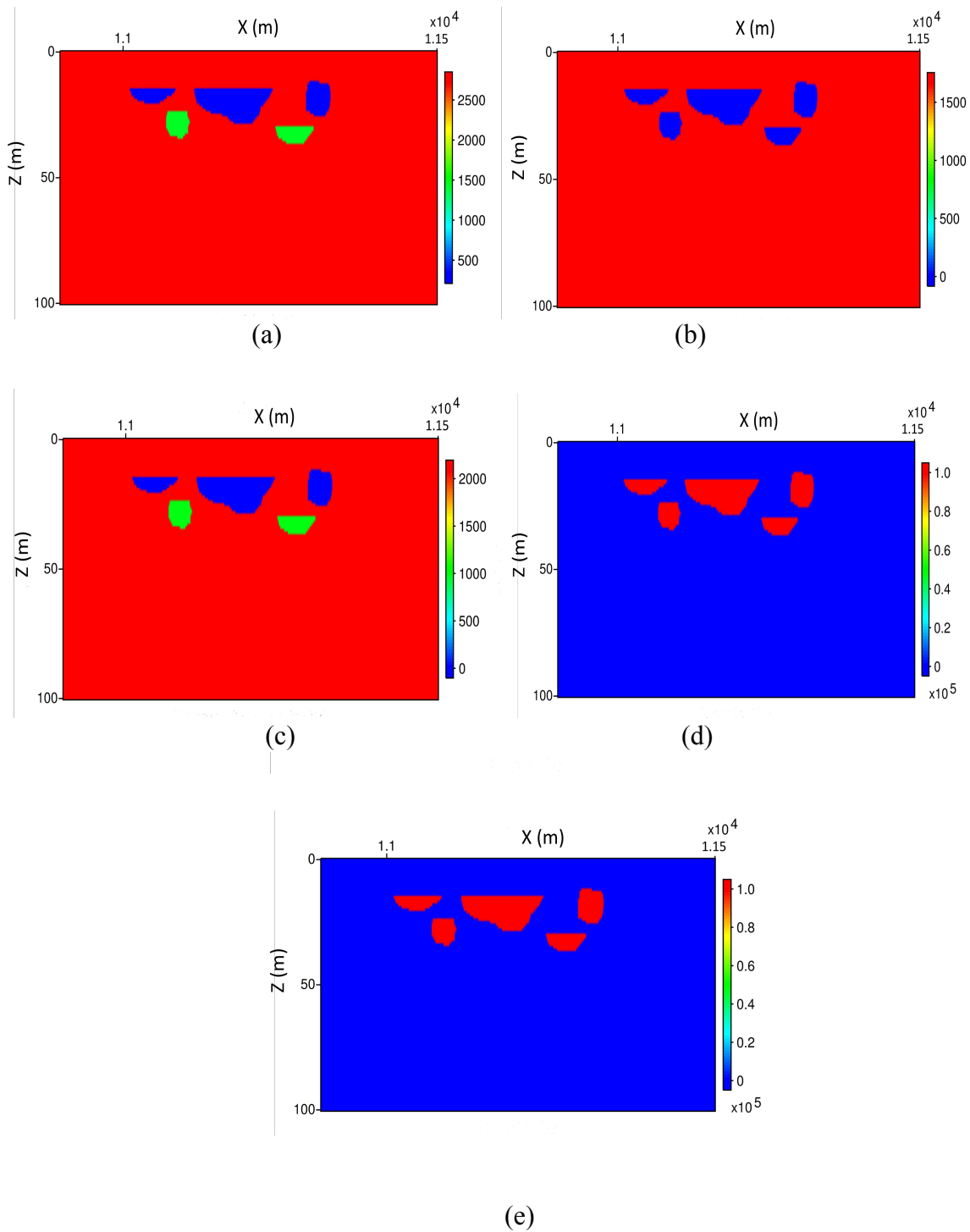


Fig. 4. (a) V_P model of the karst features in the topmost Aruma formation. (b) V_S model. (c) Density model. (d) Q_P model. (e) Q_S model. Color scales are similar to those used in Fig. 3.

GENERATION OF SYNTHETIC SEISMIC DATA

After establishing the viscoelastic properties of the two models (with and without karst features), we decimated them in order to prepare them for the generation of synthetic seismic data sets using a finite difference method (FDM). Many FDM parameters depend on the frequency content of the source wavelet. A zero-phase Ricker wavelet with a peak frequency of 25 Hz was used. The details of the parameters we used are shown in Table 3.

Table 3. Parameters used to generate the synthetic seismic data sets.

Criteria	Model without karsting	Model with karsting
Source wavelet	25-Hz zero phase Ricker	25-Hz zero phase Ricker
Time sampling for FDM calculation	0.2 msec	0.1 msec
Grid size for FDM calculation (dx = dz)	2.5 m	1 m
Receiver spacing	25 m	25 m
Shot spacing	50 m	50 m
Recording time sampling	2 msec	2 msec
Total recording time	6 sec	6 sec
Total number of receivers	801	801
Shots and receivers x-axis	0 to 20,000 m	0 to 20,000 m
Shot and receivers z-axis	-15 m	-15 m
Total number of shots	401 shots	401 shots

We made sure the selected FDM parameters satisfied the Courant–Friedrichs–Lewy (CFL) conditions of dispersion and stability necessary for the convergence of finite-difference solutions to the wave equation. We use the `fdelmodc` source code described in Thorbecke (2016) to generate the viscoelastic synthetic seismic data sets. The left, right, and bottom boundaries of the model were absorbing boundaries with a buffer area consisting of 375 grid cells beyond each of these boundaries. The top boundary was a free surface, which prompted us to put the sources and receivers 15 m below it, in order to generate and record seismic data without encountering ghost-multiple effects.

For each of the above two models (with and without karst features), two synthetic seismic data sets were generated: vertical and horizontal components. In order to simulate ambient noise effects, additive Gaussian random noise with zero mean and 10% standard deviation was added to the

synthetic data sets. Fig. 5 shows sample synthetic seismic records for both vertical and horizontal component with no karst features, while Fig. 6 shows the same records in the presence of karst features. The records of Figs. 5 and 6 have been gained using a time-squared method to enhance visibility of later arrivals. However, the uploaded digital seismic data sets are raw with no gain applied.

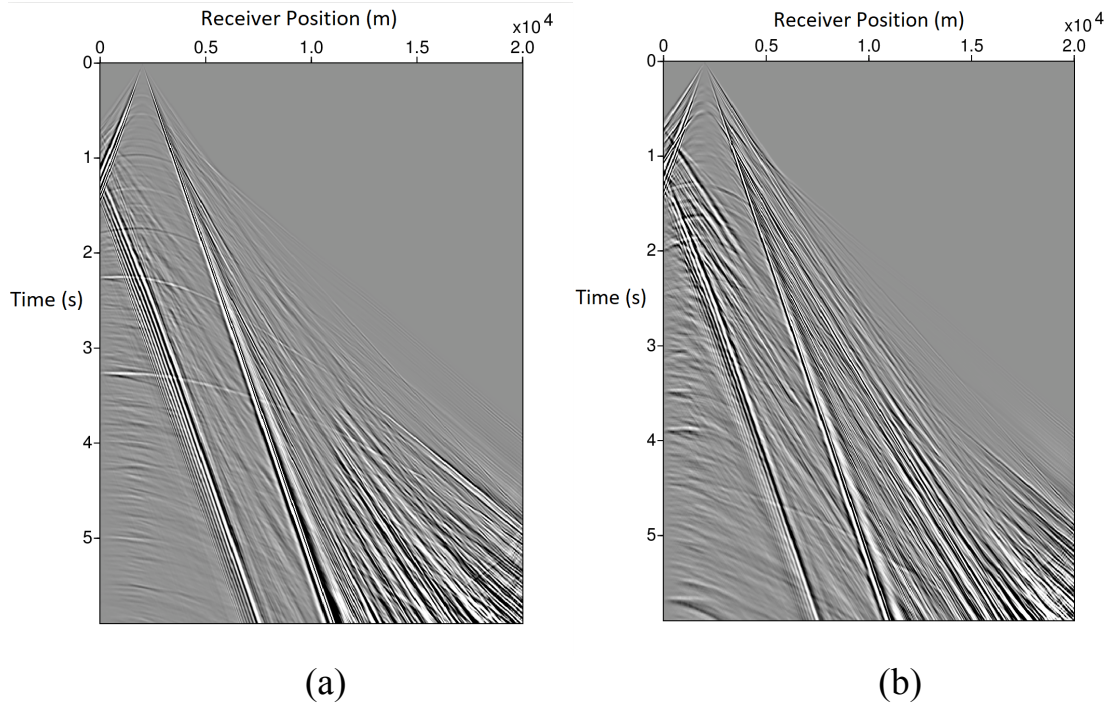


Fig. 5. (a) Horizontal component with no karst features. (b) Vertical component with no karst features.

CONCLUSION

We compiled two 2D viscoelastic seismic models (with and without karst features) of the Usaylah field of central Saudi Arabia and generated their corresponding multi-component synthetic seismic data sets. The generated models and synthetic data sets have been made available publicly over a dedicated online folder, and we invite researchers to test their algorithms on these data sets and encourage them to share their results publicly as well. We intend to extend the models to 3D geometry and include more structural, anisotropic, and fluid effects.

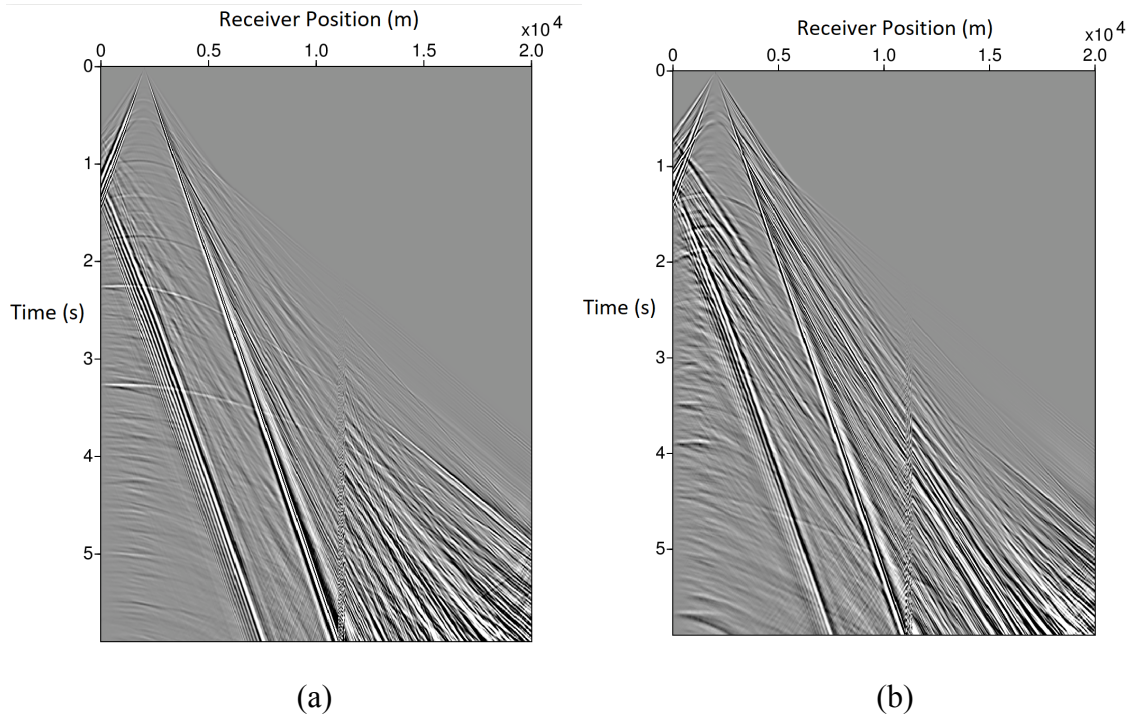


Fig. 6. (a) Horizontal component in the presence of karst features. (b) Vertical component in the presence of karst features. Note the scattering at the karst locations ($X = 11,500$ m).

ACKNOWLEDGMENTS

This work was funded by MAARIFAH – King Abdulaziz City for Science and Technology (KACST) – through the Science & Technology Unit at King Fahd University of Petroleum & Minerals (KFUPM) – the Kingdom of Saudi Arabia, award number TIC-CCS-1. We thank KACST and KFUPM for their support.

REFERENCES

- Al-Ahmadi, M.E., 2009. Hydrogeology of the Saq aquifer northwest of Tabuk northern Saudi Arabia. *Earth Sci.*, 20: 51-66.
- Alfaraj, M., Nebrija, E.L. and Ferguson, M.D. 1998. The challenge of interpreting 3-D seismic in Shaybah field Saudi Arabia. *GeoArabia*, 3: 209-226.
- Al-Husseini, M.I., 2004. Pre-Unayzah unconformity, Saudi Arabia. *GeoArabia*, 3: 15-59.
- Al-Khidir, K.E., Al-Quraishi, A.A., Al-Laboun, A.A. and Benzagouta, M.S., 2011. Bimodal pore size behavior of the Shajara Formation Reservoirs of the Permo-Carboniferous Unayzah Group, Saudi Arabia. *J. Petrol. Explor. Prod. Technol.*, 1: 1-9.

- Ameen, M.S., Smart, B.G., Somerville, J.M., Hammilton, S. and Naji, N.A., 2009. Predicting rock mechanical properties of carbonates from wireline logs (A case study: Arab-D reservoir, Ghawar field, Saudi Arabia). *Marine Petrol. Geol.*, 26: 430-444.
- Dasgupta, S.N., Hong, M.R. and Al-Jallal, I.A., 2002. Accurate characterization to reduce drilling risk in Khuff-C carbonate, Ghawar field, Saudi Arabia. *GeoArabia*, 7: 81-100.
- Evans, D.S., Bahabri, B.H. and Al-Otaibi, A.M. 1997. Stratigraphic trap in the Permian Unayzah Formation, Central Saudi Arabia. *GeoArabia*, 2: 260-278.
- Fournier, F., Dequirez, P.Y., Macridesz, C.G. and Rademakers, M., 2002. Quantitative lithostratigraphic interpretation of seismic data for characterization of the Unayzah Formation in central Saudi Arabia. *Geophysics*, 67: 1372-1381.
- Knox, R.W., Cocker, J.D. and Filatoff, J.D., 2010. Heavy mineral stratigraphy of the Unayzah Formation and Basal Khuff Clastics (Carboniferous to Permian) of Central Saudi Arabia. *GeoArabia - Middle East Petrol. Geosci.*, 15(3): 17-80.
- Liu, L., Kharji, M. and Chatterjee, H.S., 2013. Seismic attributes as exploration tools: A case study from the Jurassic in Saudi Arabia. IPTC 2013.
- Macrides, C.G. and Kelamis, P.G., 2000. 9C-2D Land seismic experiment for lithology estimation of a Permian clastic reservoir. *GeoArabia*, 5: 427-440.
- McGillivray, J.G. and Hussein, M.I., 1992. The Paleozoic petroleum geology of central Arabia. *AAPG Bull.*, 76: 1473-1490.
- Melvin, J. and Sprague, A., 2006. Origin and stratigraphic architecture of galeogenic sediments in Permian-Carboniferous Lower Unayzah Sandstones, Eastern Central Saudi Arabia. *GeoArabia* 11(4): 105-152.
- Mittet, R., 2007. A simple design procedure for depth extrapolation operators that compensate for absorption and dispersion. *Geophysics*, 72(2): S105-S112.
- Mooney, W.D., Gettings, M.E., Blank, H.R. and Healy, J.H., 1985. Saudi Arabian seismic-refraction profile: A travelttime interpretation of crustal and upper mantle structure. *Tectonophysics*, 111: 173-246.
- Thorbecke, J. 2016. 2D Finite-difference wavefield modeling. Accessed 13 Dec. 2017. <https://janth.home.xs4all.nl/Software/fdelmodcManual.pdf>.